Accepted Manuscript

Discovery of *meta*-sulfamoyl *N*-hydroxybenzamides as HDAC8 selective inhibitors

Chunlong Zhao, Jie Zang, Qin'ge Ding, Elizabeth S. Inks, Wenfang Xu, C. James Chou, Yingjie Zhang

PII: S0223-5234(18)30237-X

DOI: 10.1016/j.ejmech.2018.03.002

Reference: EJMECH 10267

To appear in: *European Journal of Medicinal Chemistry*

Received Date: 11 January 2018

Revised Date: 28 February 2018

Accepted Date: 1 March 2018

Please cite this article as: C. Zhao, J. Zang, Qin'. Ding, E.S. Inks, W. Xu, C.J. Chou, Y. Zhang, Discovery of *meta*-sulfamoyl *N*-hydroxybenzamides as HDAC8 selective inhibitors, *European Journal of Medicinal Chemistry* (2018), doi: 10.1016/j.ejmech.2018.03.002.

Graphical Abstract

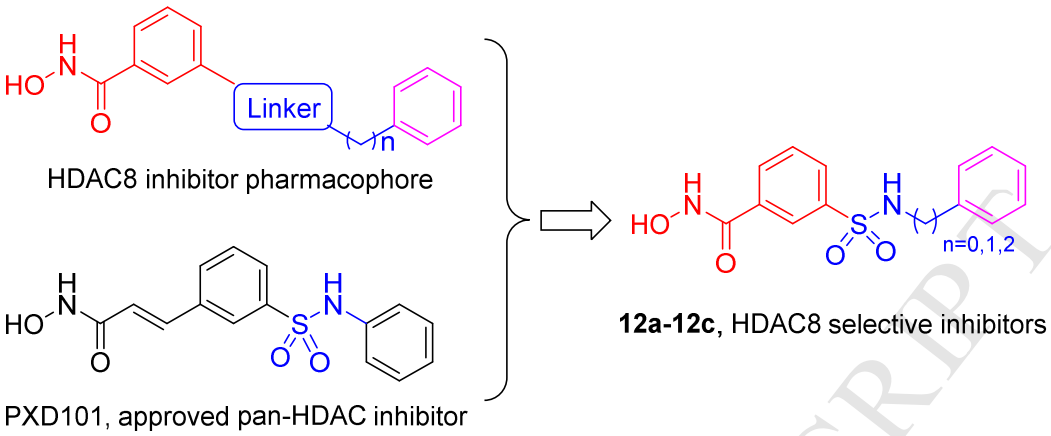

Discovery of *meta*-sulfamoyl *N*-hydroxybenzamides as HDAC8 selective inhibitors

Chunlong Zhao[1], *Jie Zang*[1], *Qin'ge Ding*[1], *Elizabeth S. Inks*[2], *Wenfang Xu*[1], *C. James Chou*[2], *Yingjie Zhang**[,1]

[1]Department of Medicinal Chemistry, Key Laboratory of Chemical Biology (Ministry of Education), School of Pharmaceutical Sciences, Shandong University, Ji'nan, Shandong, 250012, P.R. China.

[2]Department of Drug Discovery and Biomedical Sciences, South Carolina College of Pharmacy, Medical University of South Carolina, Charleston, South Carolina, 29425, United States.

*Corresponding Author. Tel/Fax: +86 531 88382009
E-mail Address: zhangyingjie@sdu.edu.cn

Abstract

In the past decade, although research and development of histone deacetylase (HDAC) inhibitors as therapeutic agents have achieved great accomplishments, especially in oncology field, there is still an urgent need for the discovery of isoform-selective HDAC inhibitors considering the side effects caused by nonselective HDAC inhibitors. HDAC8, a unique class I zinc-dependent HDAC, is becoming a potential target in cancer and other diseases. In the current study, a novel series of *N*-hydroxy-3-sulfamoylbenzamide-based HDAC8 selective inhibitors (**12a-12p**) were designed and synthesized, among which compounds **12a**, **12b** and **12c** exhibited potent HDAC8 inhibition with two-digit nanomolar IC_{50} values, and considerable selectivity over HDAC2 (> 180-fold) and HDAC6 (~30-fold) which was confirmed by western blot analysis. It is worth noting that **12a**, **12b** and **12c** displayed highly selective anti-proliferative activity to T-cell leukemia cell lines Jurkat, Molt-4 and neuroblastoma cell line SK-N-BE-(2). Such selective cytotoxicity was also observed in the well-known HDAC8 selective inhibitor PCI-34051 but not in the pan-HDAC inhibitors SAHA and PXD101, indicating that HDAC8 selective inhibitor should have preferable benefit-risk profile in comparison with pan-HDAC inhibitor. Finally, the HDAC8 selectivity of **12a**, **12b** and **12c** was rationalized by molecular docking study.

Key words: histone deacetylase, anticancer, HDAC8 inhibitor, T-cell leukemia, neuroblastoma

1. Introduction

Histone deacetylases (HDACs) are a family of enzymes that catalyze the removal of acetyl groups from N-acetyl lysine residues of histones or non-histone proteins. Thus far, 18 human HDACs have been identified and classified into 4 classes based on their homology to yeast prototypes: Class I (HDAC1, 2, 3 and 8), Class II (HDAC 4, 5, 6, 7, 9 and 10) and Class IV (HDAC11) are zinc-dependent, while Class III (SIRT1-7) is NAD^+-dependent [1, 2]. HDACs are recognized as promising therapeutic targets due to their involvement in various diseases including cancer, inflammation, neurological disorders and infections [3, 4]. To date, five HDAC inhibitors have been approved by the US Food and Drug Administration (FDA) or China FDA (CFDA) as anticancer agents: Vorinostat (SAHA), Romidepsin (FK228), Belinostat (PXD101), Panobinostat (LBH-589) and Chidamide (CS055) [2]. These approved HDAC compounds are generally considered as nonselective inhibitors which have numerous adverse effects, such as fatigue, diarrhea, low red blood cells, leukopenia, thrombopenia, and cardiac toxicity, etc, probably due to their broad-acting against the HDAC panel [5]. Therefore, there are hopes that isoform-selective HDAC inhibitors will have wider therapeutic indexes than pan- or class-selective inhibitors approved so far.

HDAC8 is a unique zinc-dependent class I HDAC, identified as a 42 kDa protein comprised of 377 amino acids and located in the nucleus and cytoplasm, where it plays numerous physiological and pathological roles [5-7]. Although it remains controversial whether histones are bona fide HDAC8 substrates, lots of non-histone proteins, such as SMC3, ERRα and p53, were reported to be either substrates or interaction partners of HDAC8 [5]. HDAC8 has been proved to be indispensable for the expression of p53. Interestingly, knockdown of HDAC8 showed anti-proliferative activity in cells with a mutant, but not wild-type p53, suggesting that HDAC8 inhibitors might function as an adjuvant therapy for tumors with mutant p53 [8]. Besides, there is increasing evidence showing that HDAC8 dysregulation plays a critical role in many diseases, especially in T-cell lymphoma, childhood neuroblastoma and Cornelia de Lange Syndrome (CdLS) [5, 9]. In the past decade, many HDAC8 selective inhibitors have been developed [10-19]. More importantly, a few HDAC8 selective inhibitors have exerted exclusive growth inhibitory effects on T-cell lymphoma and neuroblastoma cells. For example, HDAC8 selective inhibitors **1** (PCI-34051) [16], **2** [17] and **3** [18] were reported to suppress the growth of T-cell lymphoma cells, and HDAC8 selective inhibitors **2** [17], **4** [10], **5** [10] and **6** [19] displayed anti-neuroblastoma potency. Structural analysis of these reported HDCA8-selective inhibitors shown in Figure **1,** reveals that all compounds except **6** fit the common pharmacophore model where the *meta*-substituted *N*-hydroxybenzamide fragment is connected to the terminal phenyl group via various linkers (Figure **1**).

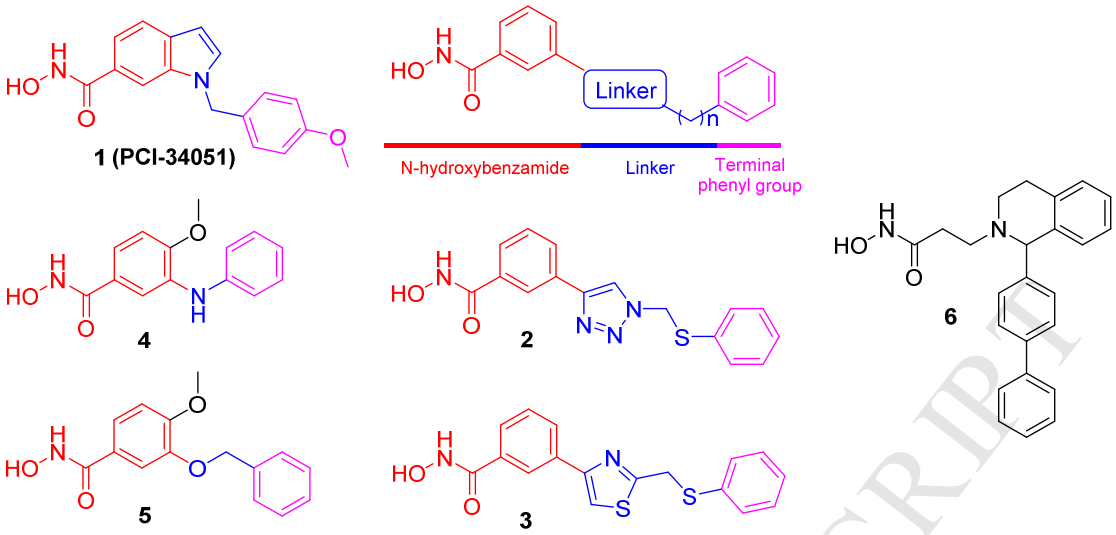

Figure **1**. HDAC8 inhibitor pharmacophore model derived from the representative selective inhibitors.

Herein, based on the above pharmacophore model of HDAC8 selective inhibitors, compounds **12a**, **12b** and **12c** were firstly designed by introducing the sulfamoyl motif as the linker between *meta*-substituted *N*-hydroxybenzamide fragment and the terminal phenyl group (Figure **2**). The sulfamoyl motif is the building block of the approved pan-HDAC inhibitor PXD101 (Figure **2**). Compared with PXD101, replacement of the *N*-hydroxycinnamamide with *N*-hydroxybenzamide might endow **12a**, **12b** and **12c** with HDAC8 selectivity. Moreover, considering the structural flexibility of the rim of HDAC8 active site [20, 21], compounds **12d-12p** were designed by replacing the phenyl group with various amino acid residues to investigate the effect of branched terminal group on HDAC8 inhibition and selectivity. Pan-HDAC inhibitory assay revealed that all synthesized compounds **12a-12p** exhibited no significant inhibition against HeLa cell nuclear extract. Further HDAC isoform selectivity evaluation showed that compounds **12a, 12b** and **12c** exhibited potent HDAC8 inhibitory activity and remarkable selectivity, which contributed to their selective cytotoxicity to T-cell leukemia cell and neuroblastoma cell lines.

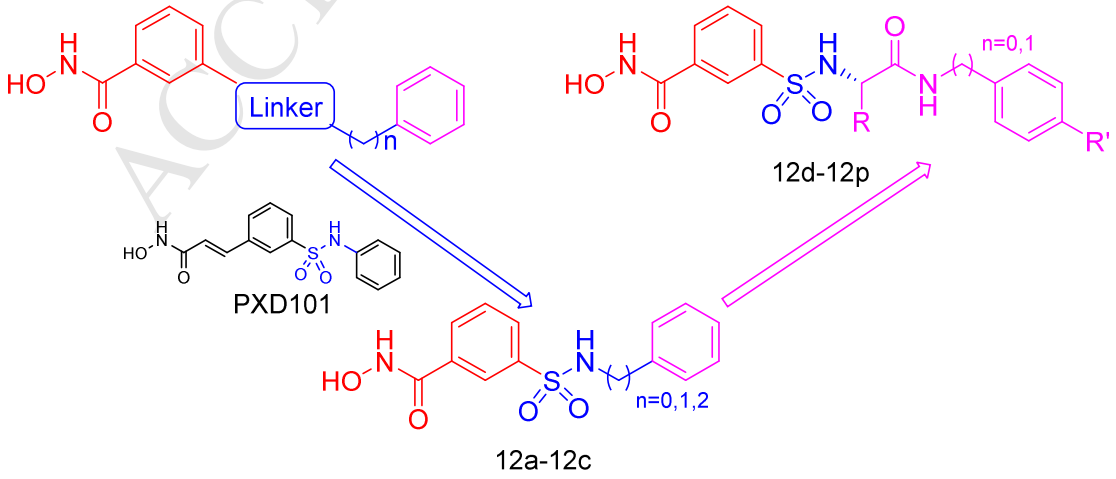

Figure **2**. Design of *meta*-sulfamoyl *N*-hydroxybenzamides-based HDAC8 inhibitors.

2. Results and discussion

2.1 Chemistry

The synthesis of compounds **12a-12p** was described in **scheme 1**. Methyl esterification of the starting material **7** led to compound **8**, which was reacted with thionyl chloride to give the key intermediate **9**. Condensation of **9** with **10a-10c** led to **11a-11c**, which were then converted to the corresponding hydroxamic acid compounds **12a-12c** with NH_2OK in methanol, respectively. Using the similar method as **12a-12c**, compounds **12d-12p** were synthesized where the intermediate **10d-10p** were obtained according to our previously described method [22].

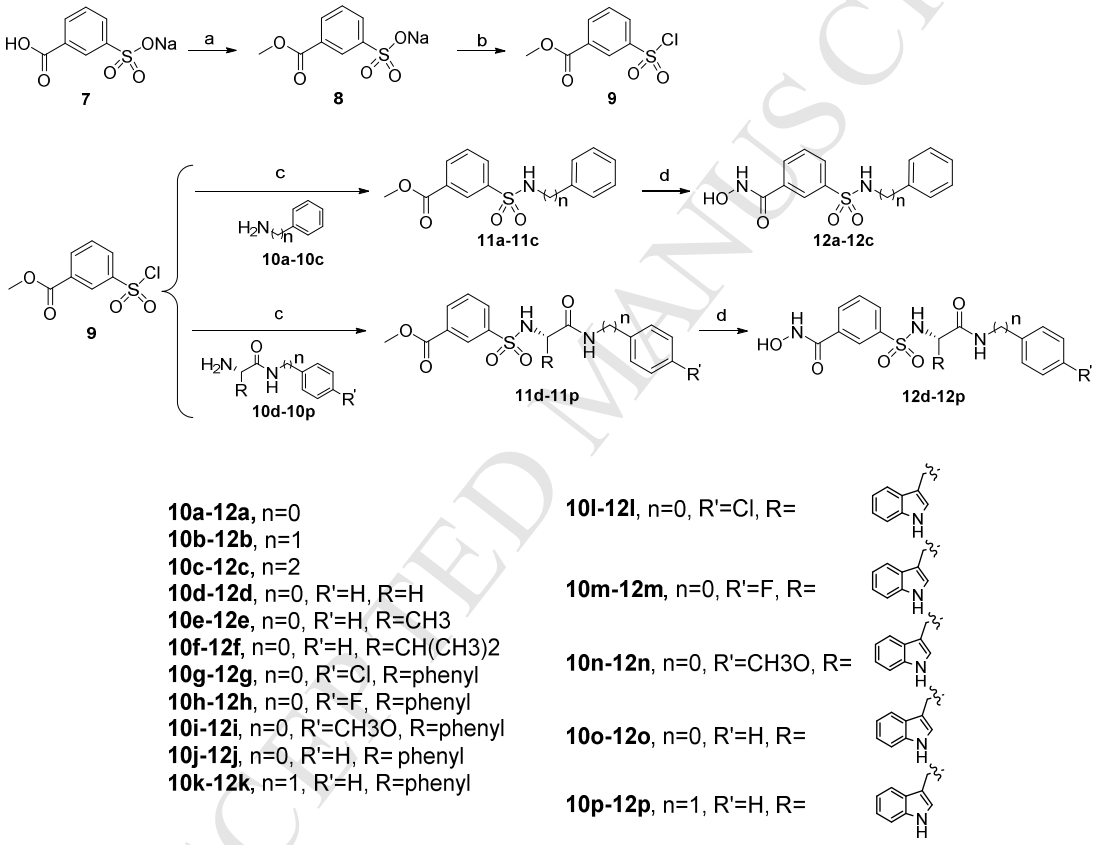

Scheme 1. Synthesis of compound**12a-12p**.

Reagents and conditions: (a) CH_3OH/HCl, $NaHCO_3$; (b) $SOCl_2$, DMF; (c) TEA, toluene; (d) KOH, $NH_2OH{\cdot}HCl$, CH_3OH

2.2 Total HDACs inhibitory assay

HeLa cell nuclear extract (mainly contains HDAC1 and 2) was selected as the enzyme source to evaluate the total HDACs inhibitory activity of our newly synthesized target compounds with SAHA and PXD101 as the positive control. Results listed in Table **1** showed that the approved pan-HDAC inhibitors SAHA and PXD101 exhibited highly potent total HDAC inhibitory activity with IC_{50} values of 0.138 μM and 0.025 μM, respectively. In contrast, all *meta*-sulfamoyl

N-hydroxybenzamides **12a-12p** exhibited no significant inhibition against HeLa cell nuclear extract at the concentration of 20 μM.

Table **1**. HDAC inhibitory activity of compounds **12a-12p**[a].

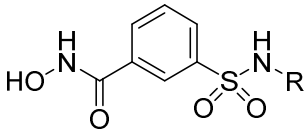

Cpd	R	IC_{50} (μM)	Cpd	R	IC_{50} (μM)
12a		> 20	**12j**	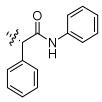	> 20
12b		> 20	**12k**	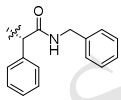	> 20
12c	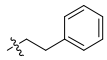	> 20	**12l**	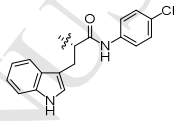	> 20
12d	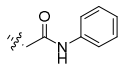	> 20	**12m**	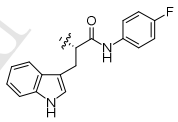	> 20
12e	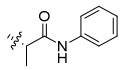	> 20	**12n**	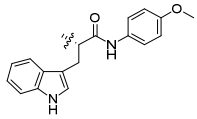	> 20
12f	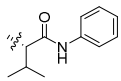	> 20	**12o**	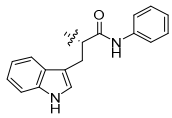	> 20
12g	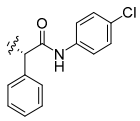	> 20	**12p**	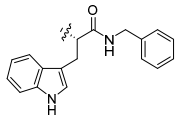	> 20
12h	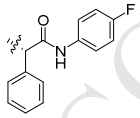	> 20	**SAHA**		0.138
12i	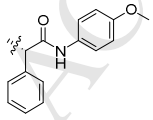	> 20	**PXD101**		0.025

[a] Assay were performed in replicate (n ≥ 3).

2.3 In vitro HDACs isoform selectivity assay

In order to explore the HDAC isoform selective profiles, several representative compounds were evaluated for their inhibitory activity against HDAC2, HDAC6 and HDAC8. Compounds **12a-12c** were selected to investigate the effect of different chain length between sulfamoyl motif and the terminal phenyl group on HDAC8 inhibition and selectivity. Compounds **12d-12f, 12j-12k** and **12o-12p** were selected to

investigate the effect of various amino acid residues on HDAC8 inhibition and selectivity. Results in Table **2** showed that compared with SAHA and PXD101, all the tested *meta*-sulfamoyl *N*-hydroxybenzamides exhibited different degrees of selectivity for HDAC8 over other tested HDAC isoforms. Among these analogs, compounds **12a, 12b** and **12c** displayed the most potent HDAC8 inhibition (IC_{50} = 0.05 μM, 0.08 μM and 0.06 μM, respectively) and considerable selectivity over HDAC2 (> 180-fold) and HDAC6 (~30-fold), validating our compound design strategy. However, introduction of branched terminal group was intolerable, leading to analogs **12d**-**12k**, **12o** and **12p** with compromised inhibitory activity towards HDAC2/6/8 and decreased selectivity for HDAC8 over HDAC6.

Table **2**. In vitro inhibition of HDAC isoforms of representative compounds[a].

Cpd	IC_{50} (μM)		
	HDAC2	**HDAC6**	**HDAC8**
12a	14.5 ± 2.4	1.5 ± 0.3	0.05 ± 0.01
12b	47.1 ± 7.0	2.6 ± 0.5	0.08 ± 0.02
12c	11.2 ± 1.8	1.8 ± 0.3	0.06 ± 0.01
12d	>100	14.1 ± 2.6	3.5 ± 0.4
12e	>100	27.7 ± 5.4	24.2 ± 3.7
12f	>100	40.5 ± 6.9	33.9 ± 4.3
12j	>100	6.7 ± 1.8	0.91 ±0.2
12k	>100	34.0 ± 5.1	9.2 ± 1.8
12o	70.4 ± 9.8	5.9 ± 1.3	3.0 ± 0.5
12p	>100	24.5 ± 4.8	19.0 ± 3.1
SAHA	0.22 ± 0.04	0.09 ± 0.02	>5
PXD101[b]	0.034±0.004 (HDAC1)	0.027±0.002	0.353±0.049

[a] Assay were performed in replicate ($n \geq 3$), values are shown as mean ± SD.

[b] Cited from Ref.[22]

2.4 Western blot analysis

Considering their remarkable HDAC8 inhibitory potency and selectivity, compounds **12a, 12b** and **12c** were progressed to western blot analysis to investigate their intracellular HDAC isoform selectivity. Results in Figure **3** revealed that compounds **12a, 12b** and **12c** had no significant influence on the intracellular levels of the HDAC6 substrate acetyl-tubulin (Ac-Tub) and the HDAC1/2/3 substrate acetyl-histone H4 (Ac-HH4). In contrast, the pan-HDAC inhibitor SAHA could dramatically increase the levels of both acetyl-tubulin and acetyl-histone H4, while the HDAC6 selective inhibitor Tubastatin A [23] could only increase the levels of acetyl-tubulin. These data was consistent with the results of HDACs isoform selectivity assay (Table **2**), indicating that compounds **12a, 12b** and **12c** had a chance to work as the HDAC8 selective inhibitors in the cellular environment.

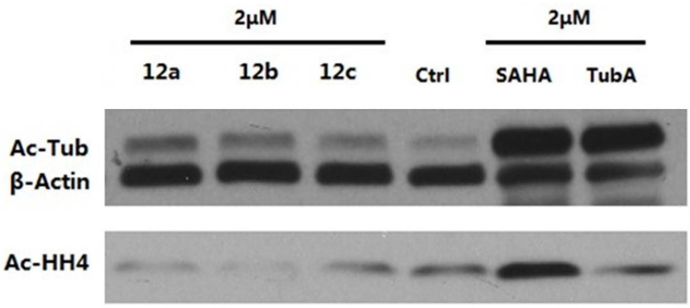

Figure **3**. Western blot analysis of acetyl-histone H4 (Ac-HH4) and acetyl-α-tubulin (Ac-Tub) in HeLa cells after 24 h treatment with compounds. β-actin was used as a loading control.

2.5 In vitro anti-proliferative activity

Based on the aforementioned results, the anti-proliferative activities of **12a, 12b** and **12c** were further evaluated, with PCI-34051, SAHA and PXD101 as the positive control. Results of MTT assays in Table **3** showed that similar to the HDAC8 selective inhibitor PCI-34051, compounds **12a, 12b** and **12c** exhibited highly selective cytotoxicity to the T-cell leukemia cell line Jurkat, the acute T-cell lymphoblastic leukemia cell line Molt-4 and the neuroblastoma cell line SK-N-BE-(2). However, such selective cytotoxicity was not observed in the pan-HDAC inhibitors SAHA and PXD101. Notably, compound **12c** showed potent anti-proliferative activity against the Jurkat and Molt-4 cell lines with IC_{50} values of 7.9 μM and 6.2 μM, respectively, which were comparable to those of PCI-34051.

Table **3**. In *vitro* anti-proliferative activity of representative compounds[a].

Cpd	**IC_{50} (μM)**						
	Jurkat	Molt-4	SK-N-BE-(2)	PC-3	HeLa	K562	HEL
12a	28.4±4.0	22.6±0.1	n.d[b]	>50	>50	>50	>50
12b	12.2±2.6	11.1±1.8	36.2±1.8	>50	>50	>50	>50
12c	7.9±1.0	6.2±0.5	25.5±0.4	>50	>50	>50	32.8±0.1
PCI-34051	4.5±0.4	9.4±1.8	16.9±1.0	19.2±1.0	>25	>25	10.8±0.9
PXD101	0.07±0.01	0.14±0.02	0.31±0.05	1.3±0.1	0.51±0.01	1.1±0.1	0.10±0.01
SAHA	0.35±0.05	0.41±0.04	2.0±0.1	6.7±0.1	1.9±0.2	0.68±0.16	0.15±0.01

[a] Assay were performed in replicate ($n \geq 3$), values are shown as mean ± SD.

[b] n.d= not determined.

2.6 Docking study

In order to rationalize their high HDAC8 selectivity, compounds **12a, 12b** and **12c** were docked into the active site of HDAC8 (PDB entry: 2V5X) and HDAC2 (PDB entry: 4LXZ), respectively. Results in Figure **4** suggested that compounds **12a** (Figure **4A**), **12b** (Figure **4B**), **12c** (Figure **4C**) and PCI-34051 (Figure **4D**) shared a similar binding model in the active pocket of HDAC8: the hydroxamic acid groups could chelate the zinc ion in a bidentate fashion and form multiple H-bond interactions with His143, His142 and Tyr306, the terminal phenyl groups tethered to

the *meta*-position of *N*-hydroxybenzamide could occupy the unique sub-pocket of HDAC8 despite their different orientation. These key interactions contributed to their potent HDAC8 inhibition. Interestingly, the sulfamoyl groups of **12a**, **12b** and **12c** showed no obvious specific interactions with HDAC8, indicating the key role of sulfamoyl group was to facilitate the terminal phenyl groups to occupy the sub-pocket. The proposed binding mode in HDAC2 revealed that, quite different with the binding mode of SAHA (Figure **5D**) where the hydroxamic acid group chelated the zinc ion strongly, the hydroxamic acid group of **12a**, **12b**, **12c** (Figure **5A**, **5B**, **5C**) projected outside the active site without chelating the zinc ion, leading to marginal HDAC2 inhibition. The lack in zinc ion chelation of **12a**, **12b** and **12c** was probably due to the steric hindrance of the *meta*-substituted sulfamoyl group, which prevented the hydroxamate group from reaching the bottom zinc ion.

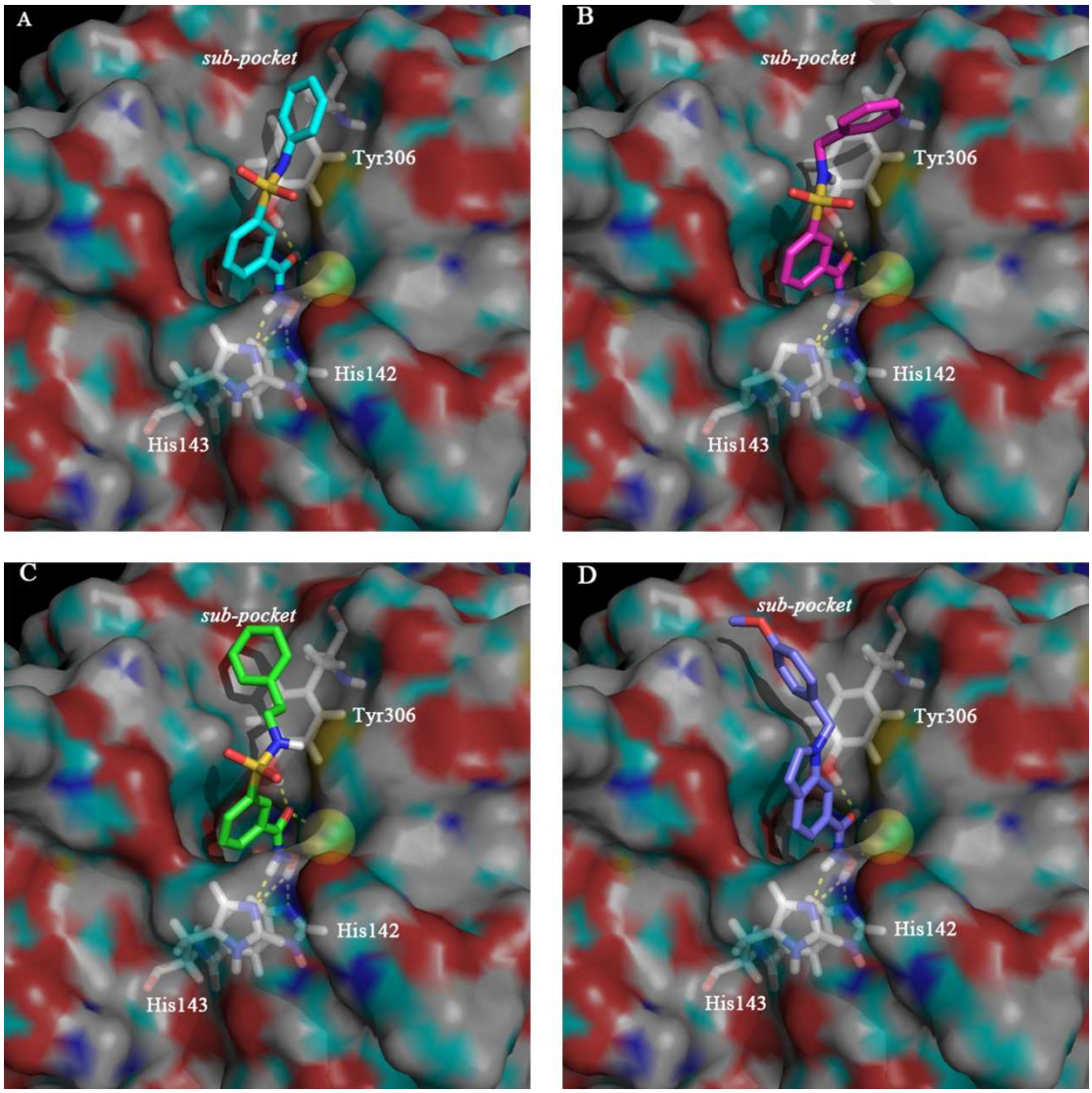

Figure **4**. Proposed binding model of compounds **12a (A)**, **12b (B)**, **12c (C)** and PCI-34051 **(D)** with HDAC8 (derived by modification of PDB code 2V5X using Tripos SYBYL-X 2.1) .The zinc ion is shown as a yellow sphere. Hydrogen bonds and coordination of the zinc ion are shown as yellow dashed lines. The figure was generated using PyMol (http://www.pymol.org/).

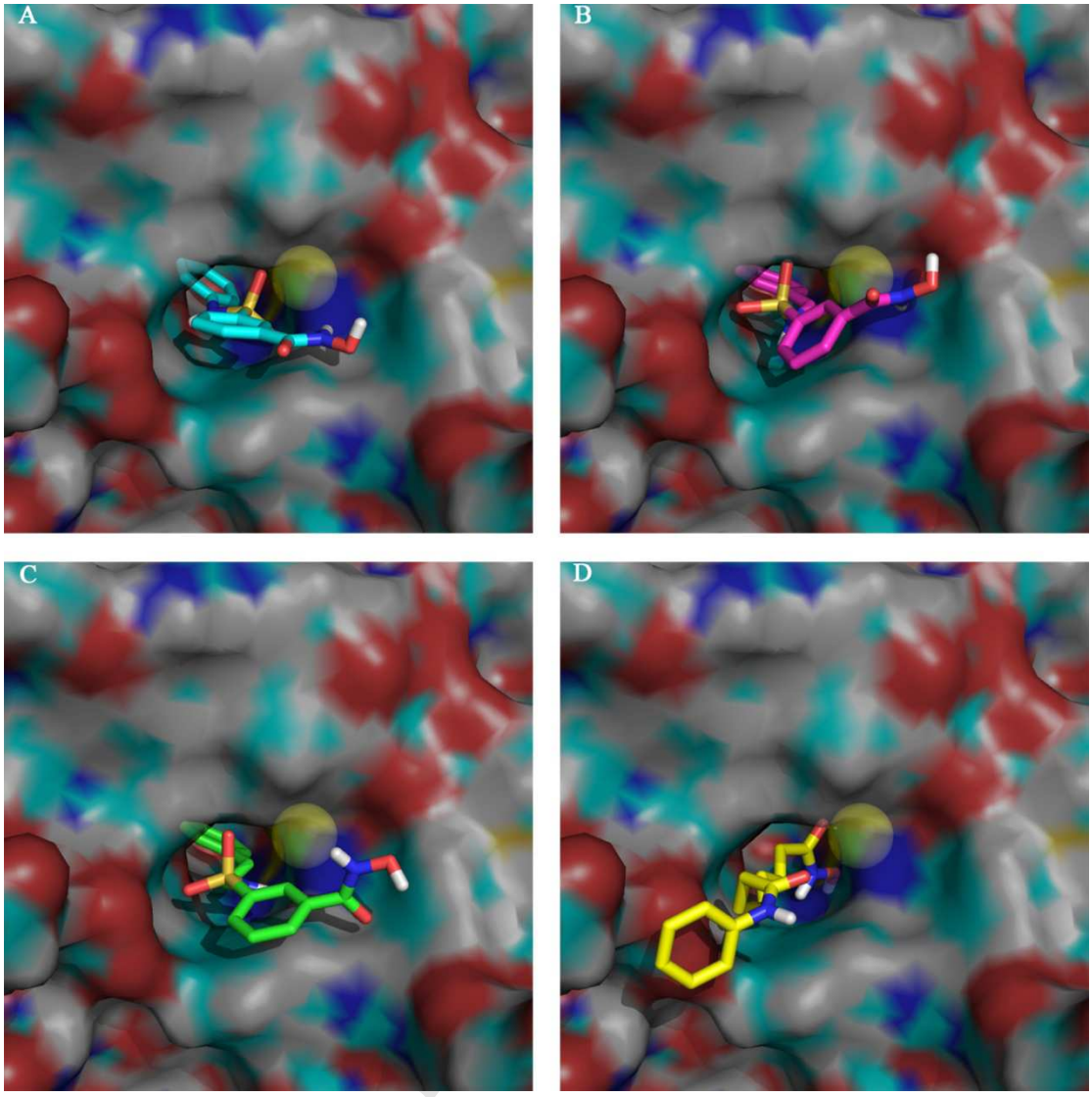

Figure **5**. Proposed binding model of compounds **12a (A)**, **12b (B)**, **12c (C)** and SAHA **(D)** with HDAC2 (derived by modification of PDB code 4LXZ using Tripos SYBYL-X 2.1). The zinc ion is shown as a yellow sphere. The figure was generated using PyMol (http://www.pymol.org/).

3. Conclusion

In the present research, the knowledge-based rational design of HDAC inhibitor led to the discovery of three *meta*-sulfamoyl *N*-hydroxybenzamide-based HDAC8 selective inhibitors **12a-12c**, which possessed selective cytotoxicity to T-cell leukemia cell lines Jurkat, Molt-4 and neuroblastoma cell line SK-N-BE-(2). Molecular docking study revealed that **12a-12c** and the well-known HDAC8 inhibitor PCI-34051 shared a similar binding mode in the active site of HDAC8, where the terminal phenyl group tethered to the *meta*-position of *N*-hydroxybenzamide via proper linker could occupy the unique sub-pocket of HDAC8. This proposed binding mode could be used to further design novel HDAC8 selective inhibitors as biological probe or therapeutic agents.

4. Experimental section

4.1. Chemistry

All commercially available starting materials, reagents and solvents were used without further purification unless otherwise stating. All reactions were monitored by thin-layer chromatography on 0.25 mm silica gel plates (60GF-254). UV light, coeruleum bromocresolis, ninhydrin, iodine stain and ferric chloride were used to visualize the spots. Anhydrous THF, CH_3OH were obtained from a distillation over sodium wire and magnesium chips, respectively. ^1H and ^{13}C NMR spectra were recorded on a Bruker DRX spectrometer at 400 MHz and 100 MHz, with δ given in parts per million (ppm) and J in hertz (Hz) and using TMS an internal standard. High-resolution spectra were performed by Shandong Analysis and Test Center in Ji'nan, China. ESI-MS spectra were recorded on an API 4000 spectrometer. Silica gel was used for column chromatography purification.

Intermediates **10d**-**10p** were synthesized according to the procedures described previously [22].

*4.1.1. sodium 3-(methoxycarbonyl)benzenesulfonate (**8**)*

Compound **7** (11.2 g, 50 mmol) was added to the mixture of anhydrous CH_3OH (145 mL) and concentrated HCl (34 mL) at room temperature. The mixture was refluxed for 4 h until the reaction was finished, then filtered to remove the white residue. The dry $NaHCO_3$ was added into the filtrate. One hour later, the mixture was filtered with the residues being washed by a small amount of CH_3OH. The filtrate was condensed under vacuum followed by addition of 135 mL of CH_3OH. After secondary filtration, the mixture was evaporated to obtain intermediate **8**, a white solid (9.8 g, 82% yield).

*4.1.2. methyl 3-(chlorosulfonyl)benzoate **(9)***

The intermediate **8** (10 g, 42 mmol) was dissolved in $SOCl_2$ (180 mL) followed by addition of 0.2 mL of DMF. Then the solution was refluxed at 80℃ for 4-6 hours. After the reaction was completed, the solution was cooled and half of the solvent was distilled off. The mixture of ice and water was added slowly into the solution at 0-5℃. After it was completely quenched, the solution was filtered and the precipitate was dried under vacuum to afford compound **9**, a white solid (8.0 g, 85% yield).

*4.1.3. General Procedure for the preparation of **11a-11p***

*4.1.3.1. Methyl 3-(N-phenylsulfamoyl)benzoate **(11a)***

To a solution of **10a** (8 g, 85.9 mmol), TEA (9.47 g, 93.7 mmol) in toluene was added a solution of **9** (10 g, 42.7 mmol) in toluene dropwise. The reaction was continued 2-3 hours at room temperature, then partial solvent was distilled off and filtered with the filter cake being washed by water and small amount of toluene to obtain **11a**, a white solid (9 g, 72% yield). ^1H NMR (400 MHz, DMSO- d_6) δ 10.41 (s, 1H), 8.31 (t, J = 1.6 Hz, 1H), 8.20–8.09 (m, 1H), 8.05–7.93(m, 1H), 7.71 (t, J = 7.8

Hz, 1H), 7.35–7.16 (m, 2H), 7.13–6.96 (m, 3H), 3.88 (s, 3H).

Compounds (**11b-11p**) were prepared using the similar procedure as **11a**.

*4.1.3.2. Methyl 3-(N-benzylsulfamoyl)benzoate **(11b)***

White solid, 65% yield. ^{1}H NMR (400 MHz, DMSO-d_6) δ 8.38 (s, 1H), 8.27 (t, *J* = 1.7 Hz, 1H), 8.15 (m, 1H), 8.06 – 7.99 (m, 1H), 7.71 (t, *J* = 7.8 Hz, 1H), 7.22 (m, 5H), 4.02 (s, 2H), 3.90 (s, 3H).

*4.1.3.3. Methyl 3-(N-phenethylsulfamoyl)benzoate **(11c)***

White solid, 67.6% yield. ^{1}H NMR (400 MHz, DMSO-d_6) δ 8.30 (t, *J* = 1.8 Hz, 1H), 8.18 (m, 1H), 8.04 (m, 1H), 7.93 (t, *J* = 5.7 Hz, 1H), 7.75 (t, *J* = 7.8 Hz, 1H), 7.29 – 7.20 (m, 2H), 7.22 – 7.09 (m, 3H), 3.91 (s, 3H), 2.98 (m, 2H), 2.67 (t, *J* = 7.4 Hz, 2H).

*4.1.3.4. Methyl 3-(N-(2-oxo-2-(phenylamino)ethyl)sulfamoyl)benzoate **(11d)***

White solid, 43% yield. ^{1}H NMR (400 MHz, DMSO-d_6) *δ* 9.96 (s, 1H), 8.50 – 8.21 (m, 2H), 8.21 – 7.99 (m, 2H), 7.73 (t, *J* = 7.8 Hz, 1H), 7.42 (d, *J* = 7.6 Hz, 2H), 7.26 (t, *J* = 7.9 Hz, 2H), 7.03 (t, *J* = 7.4 Hz, 1H), 3.85 (s, 3H), 3.73 (s, 2H).

*4.1.3.5. Methyl (S)-3-(N-(1-oxo-1-(phenylamino)propan-2-yl)sulfamoyl) benzoate **(11e)*** White solid, 60% yield. 1H NMR (400 MHz, Methanol-d_4) δ 8.44 (t, J = 1.6 Hz, 1H), 8.23 – 7.95 (m, 2H), 7.58 (t, J = 7.8 Hz, 1H), 7.24 (m, 4H), 7.11 – 6.98 (m, 1H), 4.06 (q, J = 7.1 Hz, 1H), 3.81 (s, 3H), 1.33 (d, J = 7.1 Hz, 3H).

*4.1.3.6. Methyl(S)-3-(N-(3-methyl-1-oxo-1-(phenylamino)butan-2-yl)sulfamoyl) benzoate **(11f)*** White solid, 58.6% yield. 1H NMR (400 MHz, Methanol-d_4) δ 8.43 (t, J = 1.8 Hz, 1H), 8.09 – 7.96 (m, 2H), 7.52 (t, J = 7.8 Hz, 1H), 7.18 (d, J = 5.4 Hz, 4H), 7.03 (m, 1H), 3.79 (s, 3H), 3.67 (d, J = 7.9 Hz, 1H), 1.94 (m, 1H), 1.02 (d, J = 6.7 Hz, 3H), 0.95 (d, J = 6.8 Hz, 3H).

*4.1.3.7. Methyl(S)-3-(N-(2-((4-chlorophenyl)amino)-2-oxo-1-phenylethyl)sulfamoyl) benzoate **(11g)*** White solid, 54% yield. ^{1}H NMR (300 MHz, DMSO-d_6) *δ* 10.47 (s, 1H), 9.00 (s, 1H), 8.25 (t, *J* = 1.6 Hz, 1H), 7.99 (dd, *J* = 7.9, 1.6 Hz, 2H), 7.58 (t, *J* = 7.8 Hz, 1H), 7.41–7.20 (m, 9H), 5.23 (s, 1H), 3.83 (s, 3H).

*4.1.3.8. Methyl(S)-3-(N-(2-((4-fluorophenyl)amino)-2-oxo-1-phenylethyl)sulfamoyl) benzoate **(11h)*** White solid, 68% yield. ^{1}H NMR (300 MHz, DMSO-d_6) *δ* 10.39 (s, 1H), 8.99 (s, 1H), 8.25 (t, *J* = 1.6 Hz, 1H), 8.03–7.92 (m, 2H), 7.58 (t, *J* =7.8 Hz, 1H), 7.40 – 7.20 (m, 7H), 7.08 (t, *J* = 8.9 Hz, 2H), 5.21 (s, 1H), 3.80 (s, 3H).

*4.1.3.9. Methyl(S)-3-(N-(2-((4-methoxyphenyl)amino)-2-oxo-1-phenylethyl) sulfamoyl)benzoate **(11i)*** White solid, 59% yield. ^{1}H NMR (300 MHz, DMSO-d_6) *δ* 10.18 (s, 1H), 8.95 (d, *J*= 9.2 Hz, 1H), 8.25 (t, *J* = 1.6 Hz, 1H), 8.02–7.95 (m,2H), 7.57 (t, *J* = 7.8 Hz, 1H), 7.37 (dd, *J* = 7.8, 1.7 Hz, 2H), 7.28–7.18 (m, 5H), 6.83–6.76

(m, 2H), 5.21 (s, 1H), 3.81 (s, 3H), 3.69 (s, 3H).

4.1.3.10. Methyl (S)-3-(N-(2-oxo-1-phenyl-2-(phenylamino)ethyl)sulfamoyl) benzoate ***(11j)*** White solid, 64% yield. ^{1}H NMR (300 MHz, DMSO-d_6) δ 10.31 (s, 1H), 8.99 (d, J =9.9 Hz, 1H), 8.26 (t, J = 1.6 Hz, 1H), 8.04–7.93 (m, 2H), 7.57 (t, J = 7.8 Hz, 1H), 7.38 (dd, J = 7.8, 1.6 Hz, 2H), 7.33 (d, J = 7.5 Hz, 2H), 7.23 (m, 5H), 7.02 (t, J= 7.3 Hz, 1H), 5.25 (s, 1H), 3.79 (s, 3H).

4.1.3.11. Methyl(S)-3-(N-(2-(benzylamino)-2-oxo-1-phenylethyl)sulfamoyl) benzoate ***(11k)*** White solid, 70% yield. ^{1}H NMR (300 MHz, DMSO-d_6) δ 8.87 (d, J = 9.6 Hz, 1H), 8.70 (t, J = 5.8Hz, 1H), 8.22 (t, J = 1.6 Hz, 1H), 8.15–8.02 (m, 1H), 7.96 (m, 1H), 7.59 (t, J =7.8 Hz, 1H), 7.34–7.13 (m, 8H), 7.02–6.91 (m, 2H), 5.09 (s, 1H), 4.15–3.98 (m, 2H), 3.88 (d, J =5.2 Hz, 3H).

4.1.3.12. Methyl(S)-3-(N-(1-((4-chlorophenyl)amino)-3-(1H-indol-3-yl)-1-oxopropan-2-yl)sulfamoyl)benzoate ***(11l)*** White solid, 66% yield. ^{1}H NMR (400 MHz, DMSO-d_6) δ 10.76 (d, J = 2.5 Hz, 1H), 10.20 (s, 1H), 8.55 (d, J = 8.9 Hz, 1H), 8.14 (t, J = 1.7 Hz, 1H), 7.91 – 7.81 (m, 2H), 7.45 (t, J = 7.9 Hz, 2H), 7.38 – 7.31 (m, 2H), 7.29 – 7.22 (m, 3H), 7.09 (d, J = 2.3 Hz, 1H), 7.04 – 6.99 (m, 1H), 6.94 – 6.88 (m, 1H), 4.19 (q, J = 8.0 Hz, 1H), 3.79 (s, 3H), 3.05 (dd, J = 14.5, 6.3 Hz, 1H), 2.88 (dd, J = 14.5, 8.5 Hz, 1H).

4.1.3.13. Methyl(S)-3-(N-(1-((4-fluorophenyl)amino)-3-(1H-indol-3-yl)-1-oxopropan-2-yl)sulfamoyl)benzoate ***(11m)*** White solid, 62% yield.

4.1.3.14. Methyl(S)-3-(N-(3-(1H-indol-3-yl)-1-((4-methoxyphenyl)amino)-1-oxopropan-2-yl)sulfamoyl)benzoate ***(11n)*** White solid, 58% yield. ^{1}H NMR (400 MHz, DMSO-d_6) δ 10.74 (d, J = 2.5 Hz, 1H), 9.91 (s, 1H), 8.47 (d, J = 8.8 Hz, 1H), 8.16 (t, J = 1.7 Hz, 1H), 7.86 (m, 2H), 7.49 – 7.37 (m, 2H), 7.27 – 7.16 (m, 3H), 7.08 (d, J = 2.3 Hz, 1H), 7.04 – 6.98 (m, 1H), 6.91 (t, J = 7.4 Hz, 1H), 6.82 – 6.76 (m, 2H), 4.17 (m, 1H), 3.80 (s, 3H), 3.70 (s, 3H), 3.03 (dd, J = 14.5, 6.2 Hz, 1H), 2.86 (dd, J = 14.5, 8.5 Hz, 1H).

4.1.3.15. Methyl(S)-3-(N-(3-(1H-indol-3-yl)-1-oxo-1-(phenylamino)propan-2-yl) sulfamoyl)benzoate ***(11o)*** White solid, 60% yield. 1H NMR (400 MHz, DMSO-d_6) δ 10.74 (d, J = 2.5 Hz, 1H), 10.06 (s, 1H), 8.50 (d, J = 8.6 Hz, 1H), 8.16 (t, J = 1.8 Hz, 1H), 7.92 – 7.79 (m, 2H), 7.50 – 7.39 (m, 2H), 7.37 – 7.29 (m, 2H), 7.28 – 7.17 (m, 3H), 7.09 (d, J = 2.4 Hz, 1H), 7.01 (m, 2H), 6.91 (m, 1H), 4.27 – 4.18 (m, 1H), 3.78 (s, 3H), 3.05 (m, 1H), 2.92 (m, 1H).

4.1.3.16. Methyl(S)-3-(N-(1-(benzylamino)-3-(1H-indol-3-yl)-1-oxopropan-2-yl) sulfamoyl)benzoate ***(11p)*** White solid, 57% yield. ^{1}H NMR (400 MHz, DMSO-d_6) δ 10.70 (d, J = 2.5 Hz, 1H), 8.48 (t, J = 5.8 Hz, 1H), 8.34 (s, 1H), 8.12 (t, J = 1.8 Hz, 1H), 7.96 (m, 1H), 7.77 (m, 1H), 7.44 (t, J = 7.8 Hz, 1H), 7.36 (d, J = 7.9 Hz, 1H),

7.21 (m, 4H), 7.05 – 6.93 (m, 4H), 6.87 m, 1H), 4.13 – 3.96 (m, 3H), 3.88 (s, 3H), 3.00 (dd, *J* = 14.3, 6.2 Hz, 1H), 2.79 (dd, *J* = 14.3, 8.5 Hz, 1H).

4.1.4. General Procedure for the preparation of ***12a-12p***

4.1.4.1. N-hydroxy-3-(N-phenylsulfamoyl)benzamide ***(12a)***

Compound **11a** (1.05 g, 3.61 mmol) was dissolved in the freshly prepared solution of potassium hydroxylamine (15 mL) and the mixture was stirred at room temperature for 1-2 h. The pH values of the solution was adjusted by 1 M aqueous HCl until the maximum precipitates were generated, then filtered to give 0.8 g of a brown solid, which was recrystallized from EA to give the final product **12a** as a grey solid (0.4 g), 38% yield. ^{1}H NMR (400 MHz, DMSO-d_6) δ 11.41 (s, 1H), 10.37 (s, 1H), 9.19 (s, 1H), 8.18 (t, *J* = 1.8 Hz, 1H), 7.92 (d, *J* = 7.8 Hz, 1H), 7.85 (d, *J* = 7.9 Hz, 1H), 7.62 (t, *J* = 7.8 Hz, 1H), 7.22 (t, *J* = 7.7 Hz, 2H), 7.10 – 6.99 (m, 3H). ^{13}C NMR (101 MHz, DMSO-d_6) δ 163.02, 140.42, 137.88, 134.16, 131.21, 129.99, 129.68, 129.49, 126.04, 124.75, 120.66. HRMS（AP-ESI）m/z calcd for $C_{13}H_{12}N_2O_4S$, $[M+H]^+$ 293.0596, found 293.0579.

Compounds (**12b-12p**) were prepared using the similar procedure as **12a**

4.1.4.2. 3-(N-benzylsulfamoyl)-N-hydroxybenzamide ***(12b)***

Using the synthetic method for **12a,** compound **11b** gave **12b** as a white solid, 61% yield. ^{1}H NMR (400 MHz, DMSO-d_6) δ 8.19 (d, *J* = 1.8 Hz, 1H), 7.96 (dd, *J* = 7.8, 1.5 Hz, 1H), 7.91 (m, 1H), 7.65 (t, *J* = 7.8 Hz, 1H), 7.25 (m, 5H), 4.01 (s, 2H). ^{13}C NMR (101 MHz, DMSO-d_6) δ 163.09, 141.61, 137.97, 134.22, 130.80, 129.93, 129.29, 128.69, 128.03, 127.64, 125.65, 46.56. HRMS（AP-ESI）m/z calcd for $C_{14}H_{14}N_2O_4S$, $[M+H]^+$ 307. 0753, found 307.0750.

4.1.4.3. N-hydroxy-3-(N-phenethylsulfamoyl)benzamide ***(12c)***

Using the synthetic method for **12a,** compound **11c** gave **12c** as a light brown solid, 61% yield. ^{1}H NMR (400 MHz, DMSO-d_6) δ 8.18 (d, *J* = 1.8 Hz, 1H), 7.97 (d, *J* = 7.7 Hz, 1H), 7.93 – 7.87 (m, 1H), 7.67 (t, *J* = 7.8 Hz, 1H), 7.26 (t, *J* = 7.3 Hz, 2H), 7.21 – 7.10 (m, 3H), 2.99 (t, *J* = 7.5 Hz, 2H), 2.67 (t, *J* = 7.5 Hz, 2H). ^{13}C NMR (101 MHz, DMSO-d_6) δ 163.12, 141.30, 139.07, 134.22, 130.83, 129.99, 129.34, 129.12, 128.79, 126.72, 125.67, 44.50, 35.75. HRMS:（AP-ESI）m/z calcd for $C_{15}H_{16}N_2O_4S$ $[M+H]^+$ 321.0909, found 321.0906.

4.1.4.4. N-hydroxy-3-(N-(2-oxo-2-(phenylamino)ethyl)sulfamoyl)benzamide ***(12d)***

Using the synthetic method for **12a,** compound **11d** gave **12d** as a white solid, 73% yield. ^{1}H NMR (400 MHz, DMSO-d_6) δ 11.47 (s, 1H), 9.93 (s, 1H), 9.22 (s, 1H), 8.22 (d, *J* = 9.2 Hz, 2H), 8.00 – 7.94 (m, 2H), 7.67 (t, *J* = 7.8 Hz, 1H), 7.48 (d, *J* = 8.0 Hz, 2H), 7.29 (t, *J* = 7.7 Hz, 2H), 7.04 (t, *J* = 7.4 Hz, 1H), 3.70 (d, *J* = 4.8 Hz, 2H).^{13}C-NMR(100 MHz, DMSO-*d6*) *δ* 166.62, 163.26, 141.36, 138.97, 134.04, 130.88, 129.88, 129.52, 129.20, 125.87, 123.91, 119.66, 46.20. HRMS（AP-ESI）m/z calcd for $C_{15}H_{15}N_3O_5S$ $[M+H]^+$ 350.0811, found 350.0809.

*4.1.4.5 (S)-N-hydroxy-3-(N-(1-oxo-1-(phenylamino)propan-2-yl)sulfamoyl)benzamide **(12e)***

Using the synthetic method for **12a,** compound **11e** gave **12e** as a white solid, 28% yield. ^{1}H NMR (400 MHz, DMSO-d_6) δ 11.43 (s, 1H), 9.91 (s, 1H), 9.20 (s, 1H), 8.41 (s, 1H), 8.24 (s, 1H), 7.91 (t, *J* = 8.1 Hz, 2H), 7.59 (t, *J* = 7.8 Hz, 1H), 7.41 (d, *J* = 8.0 Hz, 2H), 7.27 (t, *J* = 7.7 Hz, 2H), 7.04 (t, *J* = 7.4 Hz, 1H), 3.99 (q, *J* = 7.0 Hz, 1H), 1.17 (d, *J* = 7.0 Hz, 3H).^{13}C NMR (100 MHz, DMSO-d_6) δ 170.32, 142.02, 138.88, 133.92, 130.63, 129.70, 129.34, 129.11, 125.89, 123.98, 119.85, 52.90, 19.49. HRMS（AP-ESI）m/z calcd for $C_{16}H_{17}N_3O_5S$ $[M+H]^+$ 364.0967, found 364.0968.

*4.1.4.6.(S)-N-hydroxy-3-(N-(3-methyl-1-oxo-1-(phenylamino)butan-2-yl)sulfamoyl) benzamide **(12f)***

Using the synthetic method for **12a,** compound **11f** gave **12f** as a white solid, 37% yield. ^{1}H NMR (400 MHz, DMSO-d_6) δ 11.36 (s, 1H), 9.87 (s, 1H), 9.17 (s, 1H), 8.22 (d, *J* = 15.0 Hz, 2H), 7.86 (dd, *J* = 27.6, 7.8 Hz, 2H), 7.51 (t, *J* = 7.9 Hz, 1H), 7.32 (d, *J* = 7.9 Hz, 2H), 7.24 (t, *J* = 7.8 Hz, 2H), 7.02 (t, *J* = 7.4 Hz, 1H), 3.67 (t, *J* = 7.3 Hz, 1H), 1.89 (m, 1H), 0.84 (t, *J* = 5.3 Hz, 6H). ^{13}C NMR (100 MHz, DMSO-d_6) δ 169.33, 163.14, 142.02, 138.61, 133.66, 130.41, 129.42, 129.04, 126.02, 123.99, 119.95, 62.93, 31.36, 19.43, 18.85. HRMS（AP-ESI）m/z calcd for $C_{18}H_{21}N_3O_5S$ $[M+H]^+$ 392.1280, found 392.1271.

*4.1.4.7.(S)-3-(N-(2-((4-chlorophenyl)amino)-2-oxo-1-phenylethyl)sulfamoyl)-N-hydro xybenzamide **(12g)***

Using the synthetic method for **12a,** compound **11g** gave **12g** as a light brown solid, 40% yield. ^{1}H NMR (400 MHz, DMSO-d_6) δ 11.36 (s, 1H), 10.41 (s, 1H), 9.20 – 9.14 (m, 1H), 8.93 (d, *J* = 9.5 Hz, 1H), 8.21 (t, *J* = 1.8 Hz, 1H), 7.86 – 7.79 (m, 2H), 7.47 (t, *J* = 7.8 Hz, 1H), 7.42 – 7.34 (m, 4H), 7.33 – 7.28 (m, 2H), 7.28 – 7.19 (m, 3H), 5.19 (d, *J* = 9.4 Hz, 1H). ^{13}C-NMR (100 MHz, DMSO-d_6) δ 167.98, 163.06, 141.76, 137.58, 137.10, 133.66, 130.49, 129.41, 129.10, 128.82, 128.41, 127.83, 127.54, 126.15, 121.38, 60.62. HRMS（AP-ESI）m/z calcd for $C_{21}H_{18}ClN_3O_5S$ $[M+H]^+$ 460.0734, found 460.0726.

*4.1.4.8.(S)-3-(N-(2-((4-fluorophenyl)amino)-2-oxo-1-phenylethyl)sulfamoyl)-N-hydrox ybenzamide **(12h)***

Using the synthetic method for **12a,** compound **11h** gave **12h** as a light brown solid, 35% yield. ^{1}H NMR (400 MHz, DMSO) δ 11.44 (s, 1H), 10.53 (s, 1H), 9.15 (s, 1H), 8.90 (s, 1H), 8.23 (s, 1H), 7.96 (dd, *J* = 5.6, 4.1 Hz, 1H), 7.84 (dd, *J* = 14.8, 7.9 Hz, 1H), 7.57 – 7.34 (m, 5H), 7.29 – 7.17 (m, 3H), 7.07 (m, 2H), 5.25 (d, *J* = 10.3 Hz, 1H). HRMS（AP-ESI）m/z calcd for $C_{21}H_{18}FN_3O_5S$ $[M+H]^+$ 444.1029 ,found 444.1029.

*4.1.4.9.(S)-N-hydroxy-3-(N-(2-((4-methoxyphenyl)amino)-2-oxo-1-phenylethyl)sulfam oyl)benzamide **(12i)***

Using the synthetic method for **12a**, compound **11i** gave **12i** as a light gray solid, 60% yield. ^{1}H NMR (400 MHz, DMSO-d_6) δ 11.35 (s, 1H), 10.12 (s, 1H), 9.18 (s, 1H), 8.87 (s, 1H), 8.19 (t, *J* = 1.8 Hz, 1H), 7.82 (m, 2H), 7.46 (t, *J* = 7.8 Hz, 1H), 7.37 – 7.33 (m, 2H), 7.29 – 7.17 (m, 5H), 6.84 – 6.79 (m, 2H), 5.16 (s, 1H), 3.69 (s, 3H).^{13}C-NMR (100 MHz, DMSO-d_6) *δ* 167.34, 163.11, 156.00, 141.88, 137.52, 133.63, 131.72, 130.44, 129.38, 128.72, 128.25, 127.50, 126.11, 121.42, 114.31, 60.54, 55.61. HRMS (AP-ESI）m/z calcd for $C_{22}H_{21}N_3O_6S$ $[M+H]^+$ 456.1229, found 456.1227.

*4.1.4.10.(S)-N-hydroxy-3-(N-(2-oxo-1-phenyl-2-(phenylamino)ethyl)sulfamoyl) benzamide **(12j)***

Using the synthetic method for **12a,** compound **11j** gave **12j** as a white solid, 50% yield. ^{1}H NMR (400 MHz, DMSO-d_6) δ 11.35 (d, *J* = 1.9 Hz, 1H), 10.25 (s, 1H), 9.17 (d, *J* = 1.8 Hz, 1H), 8.88 (s, 1H), 8.19 (d, *J* = 1.8 Hz, 1H), 7.86 – 7.77 (m, 2H), 7.46 (t, *J* = 7.8 Hz, 1H), 7.40 – 7.32 (m, 4H), 7.29 – 7.16 (m, 5H), 7.06 – 6.98 (m, 1H), 5.21 (d, *J* = 9.3 Hz, 1H). ^{13}C NMR (100 MHz, DMSO- d_6) *δ* 167.85, 163.10, 141.87, 138.68, 137.36, 133.66, 130.47, 129.40, 129.19, 128.76, 128.31, 127.53, 126.11, 124.22, 119.81, 60.59. HRMS（AP-ESI）m/z calcd for $C_{21}H_{19}N_3O_5S$ $[M+H]^+$ 426.1124, found 426.1120.

*4.1.4.11.(S)-3-(N-(2-(benzylamino)-2-oxo-1-phenylethyl)sulfamoyl)-N-hydroxybenzam ide **(12k)***

Using the synthetic method for **12a,** compound **11k** gave **12k** as a white solid, 58% yield. ^{1}H-NMR：(400 MHz, DMSO- d_6) *δ* 11.44 (s, 1H), 9.20 (s, 1H), 8.74 (dd, *J* = 11.9, 6.3 Hz, 2H), 8.19 (s, 1H), 7.90 (d, *J* = 7.8 Hz, 1H), 7.84 (d, *J* = 8.0 Hz, 1H), 7.52 (t, *J* = 7.8 Hz, 1H), 7.32 (dd, *J* = 7.4, 2.0 Hz, 2H), 7.21 (m, 6H), 6.99 (d, *J* = 6.4 Hz, 2H), 5.08 (d, *J* = 7.4 Hz, 1H), 4.07 (s, 2H). ^{13}C NMR (100 MHz, DMSO- d_6) *δ* 169.18, 163.20, 141.90, 139.07, 137.99, 133.64, 130.59, 129.44, 128.70, 128.56, 128.08, 127.51, 127.47, 127.28, 126.02, 60.07, 42.52. HRMS（AP-ESI）m/z calcd for $C_{22}H_{21}N_3O_5S$ $[M+H]^+$ 440.1280, found 440.1277.

*4.1.4.12.(S)-3-(N-(1-((4-chlorophenyl)amino)-3-(1H-indol-3-yl)-1-oxopropan-2-yl)sul famoyl)-N-hydroxybenzamide **(12l)***

Using the synthetic method for **12a,** compound **11l** gave **12l** as a white solid, 40% yield. ^{1}H NMR (400 MHz, DMSO-d_6) δ 11.35 – 11.30 (m, 1H), 10.74 (d, *J* = 2.4 Hz, 1H), 10.01 (s, 1H), 9.08 (s, 1H), 8.40 (d, *J* = 8.9 Hz, 1H), 8.21 – 8.11 (m, 1H), 7.71 (m, 1H), 7.63 (m, 1H), 7.36 – 7.24 (m, 3H), 7.25 – 7.15 (m, 3H), 7.02 (d, *J* = 2.4 Hz, 1H), 6.95 (m, 1H), 6.84 (m, 1H), 4.11 (m, 1H), 3.02 (dd, *J* = 14.5, 7.0 Hz, 1H), 2.82 (dd, *J* = 14.5, 7.7 Hz, 1H). ^{13}C NMR (100 MHz, DMSO-d_6) δ 169.84, 141.71, 137.75, 136.38, 133.53, 130.40, 129.26, 129.13, 128.83, 127.54, 127.49, 125.93, 124.33, 121.50, 121.31, 118.72, 111.75, 109.36, 58.30, 29.01. HRMS（AP-ESI）m/z calcd for $C_{24}H_{21}ClN_4O_5S$ $[M+H]^+$ 513.0999, found 513.1000.

4.1.4.13.(S)-3-(N-(1-((4-fluorophenyl)amino)-3-(1H-indol-3-yl)-1-oxopropan-2-yl)sulfamoyl)-N-hydroxybenzamide ***(12m)***

Using the synthetic method for **12a,** compound **11m** gave **12m** as a light brown solid, 45% yield. ^{1}H NMR (400 MHz, DMSO-d_6) δ 11.34 (s, 1H), 10.75 (d, *J* = 2.4 Hz, 1H), 10.04 (s, 1H), 9.08 (s, 1H), 8.39 (d, *J* = 8.9 Hz, 1H), 8.14 (t, *J* = 1.8 Hz, 1H), 7.68 (m, 2H), 7.46 – 7.12 (m, 5H), 7.10 – 6.72 (m, 5H), 4.11 (m, 1H), 2.92 (m, 2H). ^{13}C NMR (100 MHz, DMSO-d_6) *δ* 169.56, 159.74, 157.35, 141.75, 136.39, 135.17, 133.52, 130.37, 129.25, 129.16, 127.56, 125.93, 124.32, 121.76, 121.69, 121.30, 118.72, 115.58, 115.36, 111.75, 109.43, 58.28, 29.04. HRMS（AP-ESI）m/z calcd for $C_{24}H_{21}FN_4O_5S$ $[M+H]^+$ 497.1295, found 497.1291.

4.1.4.14.(S)-3-(N-(3-(1H-indol-3-yl)-1-((4-methoxyphenyl)amino)-1-oxopropan-2-yl)sulfamoyl)-N-hydroxybenzamide ***(12n)***

Using the synthetic method for **12a,** compound **11n** gave **12n** as a light brown solid, 50% yield. ^{1}H NMR (400 MHz, DMSO-d_6) δ 11.42 (s, 1H), 10.82 (d, *J* = 2.5 Hz, 1H), 9.91 (s, 1H), 9.16 (s, 1H), 8.39 (d, *J* = 8.9 Hz, 1H), 8.29 – 8.18 (m, 1H), 7.81 (m, 1H), 7.71 (m, 1H), 7.47 – 7.32 (m, 2H), 7.29 (d, *J* = 8.0 Hz, 1H), 7.28 – 7.18 (m, 2H), 7.09 (d, *J* = 2.3 Hz, 1H), 7.02 (m, 1H), 6.92 (m, 1H), 6.83 – 6.74 (m, 2H), 4.17 (m, 1H), 3.70 (s, 3H), 3.08 (dd, *J* = 14.5, 7.0 Hz, 1H), 2.87 (dd, *J* = 14.5, 7.6 Hz, 1H). ^{13}C NMR (100 MHz, DMSO-d_6) *δ* 169.19, 155.80, 141.82, 136.38, 133.52, 131.92, 130.41, 129.25, 129.16, 127.59, 125.90, 124.29, 121.62, 121.27, 118.75, 118.70, 114.05, 111.73, 109.52, 58.22, 55.60, 29.14. HRMS（AP-ESI）m/z calcd for $C_{25}H_{24}N_4O_6S$ $[M+H]^+$ 509.1495, found 509.1488.

4.1.4.15.(S)-3-(N-(3-(1H-indol-3-yl)-1-oxo-1-(phenylamino)propan-2-yl)sulfamoyl)-N-hydroxybenzamide ***(12o)***

Using the synthetic method for **12a,** compound **11o** gave **12o** as a light brown solid, 38% yield. 1H NMR (400 MHz, DMSO-*d*6) δ 11.37 (s, 1H), 10.79 (s, 1H), 9.98 (s, 1H), 9.15 (s, 1H), 8.41 (d, *J* = 8.9 Hz, 1H), 8.21 (s, 1H), 7.79 (d, *J* = 7.8 Hz, 1H), 7.71 (d, *J* = 8.1 Hz, 1H), 7.41 (d, *J* = 7.9 Hz, 1H), 7.38 – 7.31 (m, 3H), 7.28 (d, *J* = 8.0 Hz, 1H), 7.22 (t, *J* = 7.9 Hz, 2H), 7.09 (d, *J* = 2.0 Hz, 1H), 7.02 (q, *J* = 7.2 Hz, 2H), 6.92 (t, *J* = 7.4 Hz, 1H), 4.19 (q, *J* = 7.5 Hz, 1H), 3.09 (dd, *J* = 14.4, 6.9 Hz, 1H), 2.87 (dd, *J* = 14.4, 7.6 Hz, 1H).^{13}C NMR (101 MHz, DMSO-d_6) δ 169.70, 163.12, 141.86, 138.81, 136.39, 133.55, 130.37, 129.25, 129.13, 128.94, 127.57, 125.89, 124.32, 123.94, 121.31, 120.06, 119.93, 118.73, 111.74, 109.45, 58.20, 29.06. HRMS（AP-ESI）m/z calcd for $C_{24}H_{22}N_4O_5S$ $[M+H]^+$ 479.1389, found 479.1389.

4.1.4.16.(S)-3-(N-(1-(benzylamino)-3-(1H-indol-3-yl)-1-oxopropan-2-yl)sulfamoyl)-N-hydroxybenzamide ***(12p)***

Using the synthetic method for **12a,** compound **11p** gave **12p** as a light brown solid, 45% yield. ^{1}H NMR (400 MHz, Methanol-d_4) δ 8.05 (t, *J* = 1.8 Hz, 1H), 7.73 (m, 1H), 7.68 (m, 1H), 7.36 – 7.31 (m, 1H), 7.30 – 7.23 (m, 2H), 7.22 – 7.14 (m, 3H), 7.04 (m, 1H), 6.96 – 6.89 (m, 4H), 4.21 (d, *J* = 15.0 Hz, 1H), 4.08 – 3.96 (m, 2H), 3.18 (dd, *J* = 14.2, 7.0 Hz, 1H), 2.91 (dd, *J* = 14.3, 7.8 Hz, 1H).^{13}C NMR (100 MHz,

DMSO-d_6) δ 170.64, 163.29, 141.89, 139.10, 136.48, 133.52, 129.30, 128.56, 127.55, 127.37, 127.04, 125.82, 124.45, 121.28, 118.72, 111.73, 109.49, 57.56, 42.39, 29.31. HRMS（AP-ESI）m/z calcd for $C_{25}H_{24}N_4O_5S$ $[M+H]^+$ 493.1546, found 493.1548.

4.2. In vitro HDACs inhibition fluorescence assay

In vitro HDACs inhibition assays were conducted as previously described [24]. In brief, 10 μL of enzyme solution (HeLa cell nuclear extract, HDAC2, HDAC6 or HDAC8) was mixed with different concentrations of tested compound (50 μL). The mixture was incubated at 37℃ for 5 mins, followed by adding 40 μL fluorogenic substrate (Boc-Lys(acetyl)-AMC for HeLa cell nuclear extracts, HDAC2 and HDAC6, Boc-Lys(triflouroacetyl)-AMC for HDAC8). After incubation at 37℃ for 30 mins, the mixture was quenched by addition of 100 μL of developer containing trypsin and Trichostatin A (TSA). Over another incubation at 37 ºC for 20 min, fluorescence intensity was measured using a microplate reader at excitation and emission wavelengths of 390 and 460 nm, respectively. The inhibition ratios were calculated from the fluorescence intensity readings of tested wells relative to those of control wells, and the IC_{50} values were calculated using a regression analysis of the concentration/inhibition data.

4.3. Western blot analysis

After compound treatment for 12 h, cells were washed twice with cold PBS and then lysed in ice-cold RIPA buffer. Lysates were cleared by centrifugation. Protein concentrations were determined using the BCA assay. Equal amounts of cell extracts were then resolved by SDS-PAGE, transferred to nitrocellulose membranes and probed with ac-histone H4 antibody, ac-tubulin antibody and β-actin antibody, respectively. Blots were detected using an ECL system.

4.4. In vitro anti-proliferative assay

All cell lines were maintained in RPMI1640 medium containing 10% FBS at 37℃ in a 5% CO_2 humidified incubator. Cell proliferation assay was determined by the MTT (3-[4,5-dimethyl-2-thiazolyl]-2,5-diphenyl-2h-tetrazolium bromide) method. Briefly, cells were passaged the day before dosing into a 96-well plate, allowed to grow for 12 h, and then treated with different concentrations of compound for 48 h. A 0.5% MTT solution was added to each well. After incubation for another 4 h, formazan formed from MTT was extracted by adding 150 uL of DMSO. Absorbance was then determined using an ELISA reader at 570 nm.

4.5. Molecular docking studies

Compounds were docked into the active site of HDAC8 (PDB entry: 2V5X) and HDAC2 (PDB entry: 4LZX) using Tripos SYBYL-X 2.1. Before docking process, the protein structure retrieved from PDB site was treated by deleting water molecules, FF99 charges. A 100-step minimization process was performed to further optimize the protein structure. The molecular structures were generated with Sybyl/Sketch module and optimized using Powell’s method with the Tripos force field with convergence

criterion set at 0.05 kcal/(Å mol) and assigned charges with the Gasteiger_Hückel method. Molecular docking was carried out via the Sybyl/Surflex-Dock module. Other docking parameters were kept to the default values.

Acknowledgement

This work was supported by Young Scholars Program of Shandong University (YSPSDU, Grant No. 2016WLJH33), Natural Science Foundation of Shandong Province (Grant No. ZR201709190013), Major Project of Science and Technology of Shandong Province (Grant No. 2015ZDJS04001, 2017CXGC1401).

References

[1] M. Yoshida, N. Kudo, S. Kosono, A. Ito, Chemical and structural biology of protein lysine deacetylases, Proceedings of the Japan Academy. Series B, Physical and biological sciences, 93 (2017) 297-321.

[2] C. Zagni, G. Floresta, G. Monciino, A. Rescifina, The Search for Potent, Small-Molecule HDACIs in Cancer Treatment: A Decade After Vorinostat, Med Res Rev, 37 (2017) 1373-1428.

[3] K.J. Falkenberg, R.W. Johnstone, Histone deacetylases and their inhibitors in cancer, neurological diseases and immune disorders, Nat Rev Drug Discov, 13 (2014) 673-691.

[4] G.S. Clemens Zwergel, Sergio Valente and Antonello Mai, Histone Deacetylase Inhibitors: Updated Studies in Various Epigenetc-Related Diseases, Journal of Clinical Epigenetics, 2 (2016) 1-15.

[5] J.M. Alokta Chakrabarti, Fiona R Kolbinger, Ina Oehme, Johanna Senger, Olaf Witt, Wolfgang Sippl & Manfred Jung, Targeting histone deacetylase 8 as a therapeutic approach to cancer and neurodegenerative diseases, Future Medicinal Chemistry, 8 (2016) 1609-1634.

[6] E. Hu, Z. Chen, T. Fredrickson, Y. Zhu, R. Kirkpatrick, G.F. Zhang, K. Johanson, C.M. Sung, R. Liu, J. Winkler, Cloning and characterization of a novel human class I histone deacetylase that functions as a transcription repressor, J Biol Chem, 275 (2000) 15254-15264.

[7] J. Li, S. Chen, R.A. Cleary, R. Wang, O.J. Gannon, E. Seto, D.D. Tang, Histone deacetylase 8 regulates cortactin deacetylation and contraction in smooth muscle tissues, Am J Physiol Cell Physiol, 307 (2014) C288-295.

[8] W. Yan, S. Liu, E. Xu, J. Zhang, Y. Zhang, X. Chen, X. Chen, Histone deacetylase inhibitors suppress mutant p53 transcription via histone deacetylase 8, Oncogene, 32 (2013) 599-609.

[9] A. Chakrabarti, I. Oehme, O. Witt, G. Oliveira, W. Sippl, C. Romier, R.J. Pierce, M. Jung, HDAC8: a multifaceted target for therapeutic interventions, Trends Pharmacol Sci, 36 (2015) 481-492.

[10] T. Heimburg, F.R. Kolbinger, P. Zeyen, E. Ghazy, D. Herp, K. Schmidtkunz, J. Melesina, T.B. Shaik, F. Erdmann, M. Schmidt, C. Romier, D. Robaa, O. Witt, I. Oehme, M. Jung, W. Sippl, Structure-Based Design and Biological Characterization of Selective Histone Deacetylase 8 (HDAC8) Inhibitors with Anti-Neuroblastoma Activity, J Med Chem, 60 (2017) 10188-10204.

[11] O.J. Ingham, R.M. Paranal, W.B. Smith, R.A. Escobar, H. Yueh, T. Snyder, J.A. Porco, Jr., J.E. Bradner, A.B. Beeler, Development of a Potent and Selective HDAC8 Inhibitor, ACS Med Chem Lett, 7 (2016) 929-932.

[12] A. Kleinschek, C. Meyners, E. Digiorgio, C. Brancolini, F.J. Meyer-Almes, Potent and Selective Non-hydroxamate Histone Deacetylase 8 Inhibitors, ChemMedChem, 11 (2016) 2598-2606.

[13] U. Kulandaivelu, L.M. Chilakamari, S.S. Jadav, T.R. Rao, K.N. Jayaveera, B. Shireesha, A.T. Hauser, J. Senger, M. Marek, C. Romier, M. Jung, V. Jayaprakash, Hydroxamates of para-aminobenzoic acid as

selective inhibitors of HDAC8, Bioorg Chem, 57 (2014) 116-120.

[14] P. Galletti, A. Quintavalla, C. Ventrici, G. Giannini, W. Cabri, S. Penco, G. Gallo, S. Vincenti, D. Giacomini, Azetidinones as zinc-binding groups to design selective HDAC8 inhibitors, ChemMedChem, 4 (2009) 1991-2001.

[15] K. Krennhrubec, B.L. Marshall, M. Hedglin, E. Verdin, S.M. Ulrich, Design and evaluation of 'Linkerless' hydroxamic acids as selective HDAC8 inhibitors, Bioorg Med Chem Lett, 17 (2007) 2874-2878.

[16] S. Balasubramanian, J. Ramos, W. Luo, M. Sirisawad, E. Verner, J.J. Buggy, A novel histone deacetylase 8 (HDAC8)-specific inhibitor PCI-34051 induces apoptosis in T-cell lymphomas, Leukemia, 22 (2008) 1026-1034.

[17] T. Suzuki, Y. Ota, M. Ri, M. Bando, A. Gotoh, Y. Itoh, H. Tsumoto, P.R. Tatum, T. Mizukami, H. Nakagawa, S. Iida, R. Ueda, K. Shirahige, N. Miyata, Rapid discovery of highly potent and selective inhibitors of histone deacetylase 8 using click chemistry to generate candidate libraries, J Med Chem, 55 (2012) 9562-9575.

[18] T. Suzuki, N. Muto, M. Bando, Y. Itoh, A. Masaki, M. Ri, Y. Ota, H. Nakagawa, S. Iida, K. Shirahige, N. Miyata, Design, synthesis, and biological activity of NCC149 derivatives as histone deacetylase 8-selective inhibitors, ChemMedChem, 9 (2014) 657-664.

[19] T.Y. Taha, S.M. Aboukhatwa, R.C. Knopp, N. Ikegaki, H. Abdelkarim, J. Neerasa, Y. Lu, R. Neelarapu, T.W. Hanigan, G.R.J. Thatcher, P.A. Petukhov, Design, Synthesis, and Biological Evaluation of Tetrahydroisoquinoline-Based Histone Deacetylase 8 Selective Inhibitors, ACS Med Chem Lett, 8 (2017) 824-829.

[20] N. Deschamps, C.A. Simoes-Pires, P.A. Carrupt, A. Nurisso, How the flexibility of human histone deacetylases influences ligand binding: an overview, Drug Discov Today, 20 (2015) 736-742.

[21] G. Estiu, N. West, R. Mazitschek, E. Greenberg, J.E. Bradner, O. Wiest, On the inhibition of histone deacetylase 8, Bioorg Med Chem, 18 (2010) 4103-4110.

[22] J. Li, X. Li, X. Wang, J. Hou, J. Zang, S. Gao, W. Xu, Y. Zhang, PXD101 analogs with L-phenylglycine-containing branched cap as histone deacetylase inhibitors, Chem Biol Drug Des, 88 (2016) 574-584.

[23] J.K. Kyle V. Butler, Camille Brochier, Guilio Vistoli, Brett Langley, and Alan P. Kozikowski, Rational Design and Simple Chemistry Yield a Superior, Neuroprotective HDAC6 Inhibitor, Tubastatin A, Journal of the American Chemical Society, 132 (2010) 10842-10846.

[24] X. Li, E.S. Inks, X. Li, J. Hou, C.J. Chou, J. Zhang, Y. Jiang, Y. Zhang, W. Xu, Discovery of the first N-hydroxycinnamamide-based histone deacetylase 1/3 dual inhibitors with potent oral antitumor activity, J Med Chem, 57 (2014) 3324-3341.

Highlights

> Novel *N*-hydroxy-3-sulfamoylbenzamide-based HDAC8 inhibitors were discovered.

> 12a-**12c** exhibited potent HDAC8 inhibition and remarkable selectivity over HDAC2/6.

> 12a-**12c** were selectively cytotoxic to Jurkat, Molt-4 and SK-N-BE-(2) cell lines.